

# Novel aspects of particle production in ultra-peripheral collisions

F.C. Sobrinho<sup>1</sup>, L.M. Abreu<sup>1,2</sup>, C.A. Bertulani<sup>3,4</sup>, I. Danhoni<sup>4</sup>, F.S. Navarra<sup>1</sup>

<sup>1</sup>Instituto de Física, Universidade de São Paulo, Rua do Matão 1371, Cidade Universitária, - 05508-090, São Paulo, SP, Brazil

<sup>2</sup>Instituto de Física, Universidade Federal da Bahia, Campus Ondina - 40170-115, Salvador, Bahia, Brazil

<sup>3</sup>Department of Physics and Astronomy, Texas A&M University-Commerce, Commerce, Texas 75429, USA

<sup>4</sup>Institut für Kernphysik, Technische Universität Darmstadt, 64289 Darmstadt, Germany

One of the hot topics in hadron physics is the study of the new exotic charmonium states and the determination of their internal structure. Another important topic is the study of the magnetic field produced in relativistic heavy ion collisions and its effects on observables. In this note we show that we can use ultra-peripheral collisions to address both topics. We compute the cross section for the production of the  $D^+D^-$  molecular bound state in photon-photon collisions and also the cross section for  $\pi^0$  production in the target induced by the magnetic field of the projectile. Both cross sections are sizeable and their measurement would be very useful to elucidate the above mentioned questions.

DOI: <https://doi.org/10.17161/d02wbn61>

*Keywords:* ultra-peripheral collisions, exotic charmonium, strong magnetic field

## 1 Introduction

In ultra-peripheral collisions (UPCs) target and projectile do not overlap and stay intact. As a consequence only few particles are produced, the background is reduced and we can study more carefully specific particle production processes, such as those addressed here. These features have been explored at the large hadron collider (LHC) at CERN and at the relativistic heavy ion collider (RHIC) at Brookhaven. In UPCs the elementary processes which contribute to particle production are photon-photon, photon-Pomeron and Pomeron-Pomeron fusion. They are a good environment to search for particles which are more difficult to identify in central collisions<sup>1</sup>.

In this work we discuss two processes of particle production, which may be studied in UPCs: production of  $D^+D^-$  meson molecules and production of forward pions. In the first we can gain some insight on the nature of these exotic charmonium states and in the second we can measure the magnetic field produced by relativistic heavy ions. In the next section we briefly describe the formalism employed to study the production of charm molecules, in the following section we address forward pion production and at the end we present some conclusions.

## 2 Production of charm meson molecules

One important research topic in modern hadron physics is the study of the exotic charmonium states<sup>2</sup>. These new mesonic states are not conventional  $c\bar{c}$  configurations and their minimum quark content is  $c\bar{c}q\bar{q}$ . The main question in the field is: are these multiquark states compact tetraquarks or are they large and loosely bound meson molecules? Perhaps the largest fraction of the community tends to believe that they are molecules. One of the frequently invoked arguments is that the masses of almost all these states are very close to thresholds, i.e. to the sum of the masses of two well known meson states<sup>2,3,4</sup>. A genuine tetraquark state could in principle have any mass, including masses far from thresholds. Besides, some problems have been detected in the calculation of tetraquark masses with QCD sum rules<sup>5,6</sup>. Nevertheless, so far there is no conclusive answer.

The production of hadron molecules has been discussed in the context of B decays<sup>3</sup>, in  $e^+e^-$  collisions, in proton-proton<sup>4,7,8</sup>, in proton-nucleus, in central nucleus-nucleus collisions<sup>9</sup> and also in UPCs<sup>10</sup>. In

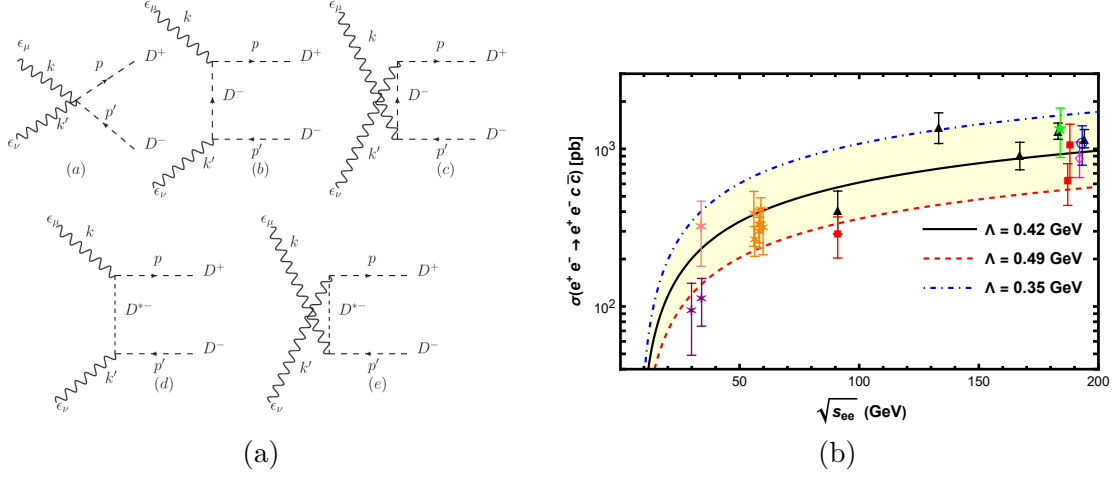


Figure 1 – a) Feynman diagrams for the process  $\gamma\gamma \rightarrow D^+D^-$ . b) Cross sections of the process  $e^+e^- \rightarrow e^+e^- c\bar{c}$  as a function of the energy  $\sqrt{s}$ . Points are a compilation of LEP data published in arXiv:hep-ex/0010060 [hep-ex]. Lines represent the results obtained with Eq.(15) adapted to  $e^+e^- \rightarrow e^+e^- D^+D^-$ .

this section we focus on the  $D^+D^-$  molecule production in UPCs, but the method employed here is applicable to all molecular states.

The  $D^+D^-$  pair is produced from two photons. This process can be described by well known hadronic effective Lagrangians, from which we obtain the pair production amplitude. This amplitude is subsequently projected onto the amplitude for bound state formation. If the properties of the bound state are known, the only unknown in this formalism is the form factor, which must be attached to the vertices to account for the finite size of the hadrons.

We will study the process  $\gamma\gamma \rightarrow D^+D^-$  with the Lagrangian densities<sup>11</sup>

$$\mathcal{L} = (D_\mu\phi)^*(D^\mu\phi) - m_D^2\phi^*\phi - \frac{1}{4}F_{\mu\nu}F^{\mu\nu}, \quad (1)$$

and

$$\mathcal{L} = -ig_{\gamma D^+D^*} F_{\mu\nu}\epsilon^{\mu\nu\alpha\beta}(D_\alpha^* - \partial_\beta D^+ - \partial_\beta D_\alpha^* D^+ + D^- \partial_\beta D_\alpha^* - \partial_\beta D^- D_\alpha^*), \quad (2)$$

where

$$D_\mu\phi = \partial_\mu\phi + ieA_\mu\phi, \quad F_{\mu\nu} = \partial_\mu A_\nu - \partial_\nu A_\mu, \quad (3)$$

and  $\phi$ ,  $D^*$  and  $A_\mu$  represent the pseudoscalar charm meson (with mass  $m_D$ ), the vector charm meson (with mass  $m_{D^*}$ ) and the photon field, respectively. The Feynman rules can be derived from the interaction terms and they yield the Feynman diagrams for the process  $\gamma\gamma \rightarrow D^+D^-$  shown in Fig. 1a. In the figure we also show the quadrimomenta of the incoming photons  $k^\mu = (E_p, 0, 0, \mathbf{k})$ ,  $k'^\mu = (E_{k'}, 0, 0, \mathbf{k}')$  and of the outgoing mesons  $p^\mu = (E_p, 0, 0, \mathbf{p})$ ,  $p'^\mu = (E_{p'}, 0, 0, \mathbf{p}')$ . The scattering amplitude can be derived from the Feynman rules.

As usual, we include form factors,  $F(q)$ , in the vertices of the amplitudes. We shall follow<sup>12</sup> and use the monopole form factor given by

$$F(q^2) = \frac{\Lambda^2 - m_{D^{(*)}}^2}{\Lambda^2 - q^2}, \quad (4)$$

where  $q$  is the 4-momentum of the exchanged meson and  $\Lambda$  is a cut-off parameter. This choice has the advantage of yielding automatically  $F(m_D^2) = 1$  and  $F(m_{D^*}^2) = 1$  when the exchanged meson is on-shell. The above form is arbitrary but there is hope to improve this ingredient of the calculation using QCD sum rules to calculate the form factor, as done in<sup>13</sup>, thereby reducing the uncertainties. Taking the square of the amplitude and the average over the photon polarizations it is straightforward to calculate the cross section:

$$\sigma = \frac{1}{64\pi^2} \frac{1}{\hat{s}} \sqrt{1 - \frac{4m_D^2}{\hat{s}}} \int |M(\gamma\gamma \rightarrow D^+D^-)|^2 d\Omega. \quad (5)$$

where  $\hat{s} = (k+k')^2$ . We emphasize that the only unknown in our calculation is the cut-off parameter  $\Lambda$ . In what follows, we will determine it fitting our cross section to the LEP data on the process  $e^+e^- \rightarrow e^+e^- c\bar{c}$ .

From the  $D^+D^-$  pair we can construct a bound state (denoted  $B$ ). As in<sup>4</sup>, we impose phase space constraints on the mesons, forcing them to be “close together”. Here we do this through the prescription discussed in<sup>14</sup>. The bound state  $|B\rangle$  is defined as

$$\frac{|B\rangle}{\sqrt{2E_B}} \equiv \int \frac{d^3q}{(2\pi)^3} \tilde{\psi}^*(\mathbf{q}) \frac{1}{\sqrt{2E_q}} \frac{1}{\sqrt{2E_{-q}}} |\mathbf{q}, -\mathbf{q}\rangle, \quad (6)$$

where  $E_B$  is the bound state energy,  $\mathbf{q}$  is the relative three momentum between  $D^+$  and  $D^-$  in the state  $B$ ,  $E_{\pm q}$  are the energies of  $D^+$  and  $D^-$  and  $\tilde{\psi}(\mathbf{q})$  is the bound state wave function in momentum space. From Eq. (6), we can write the following relation between the amplitudes:

$$\frac{M(\gamma\gamma \rightarrow B)}{\sqrt{2E_B}} = \int \frac{d^3q}{(2\pi)^3} \tilde{\psi}^*(\mathbf{q}) \frac{1}{\sqrt{2E_{D^+}}} \frac{1}{\sqrt{2E_{D^-}}} M(\gamma\gamma \rightarrow D^+D^-), \quad (7)$$

We assume that the  $\mathbf{p} \simeq \mathbf{p}'$  and hence  $E_{D^+} \simeq E_{D^-} = E_D$ . Consequently, the relative momentum  $\mathbf{q} = \mathbf{p} - \mathbf{p}'$  is close to zero. Therefore the energy  $E_D$  and the amplitude  $M(\gamma\gamma \rightarrow D^+D^-)$  depend only weakly on  $\mathbf{q}$  and can be taken out of the integral. Moreover, since the binding energy is small we have  $E_B \simeq 2E_D$  and hence

$$M(\gamma\gamma \rightarrow B) = \psi^*(0) \sqrt{\frac{2}{E_B}} M(\gamma\gamma \rightarrow D^+D^-). \quad (8)$$

With the amplitude above we calculate the cross section for bound state production:

$$d\sigma = \frac{1}{H} \frac{d^3p_B}{(2\pi)^3} \frac{1}{2E_B} (2\pi)^4 \delta^{(4)}(k + k' - p_B) |M(\gamma\gamma \rightarrow B)|^2, \quad (9)$$

where  $p_B$  is the momentum of the produced bound state and  $H$  is the flux factor. In the center of mass frame of the  $AA \rightarrow AAB$  collision, we have

$$k = (\omega_1, 0, 0, \omega_1), \quad k' = (\omega_2, 0, 0, -\omega_2), \quad p_B \equiv p + p' = (E_B, 0, 0, \omega_1 - \omega_2), \quad (10)$$

where  $E_B = \sqrt{(\omega_1 - \omega_2)^2 + m_B^2}$  and  $\omega_1$  and  $\omega_2$  are the energies of the colliding photons. The flux factor is then given by  $H = 8\omega_1\omega_2$ . The integrated cross section reads:

$$\sigma(\omega_1, \omega_2) = \frac{2\pi}{2(4\omega_1\omega_2)} \int \frac{d^3p_B}{2E_B} \delta(E_{CM} - E_B) \delta^{(3)}(\mathbf{k} + \mathbf{k}' - \mathbf{p}_B) \left[ \frac{2}{E_B} |\psi(0)|^2 |M(\gamma\gamma \rightarrow D^+D^-)|^2 \right] \quad (11)$$

where  $E_{CM}^2 = 4\omega_1\omega_2$ . To complete the calculation we need the bound state wave function at the origin  $|\psi(0)|^2$ . In<sup>15</sup> a similar bound state of open charm mesons was studied with the Bethe-Salpeter equation and an expression for the wave function was derived. Here we will just quote the final expression needed to calculate  $\psi(0)$ , which is given by:

$$\psi(0) = \frac{-8\mu\pi g}{(2\pi)^{3/2}} \left( \Lambda_0 - \sqrt{2\mu E_b} \arctan \left( \frac{\Lambda_0}{\sqrt{2\mu E_b}} \right) \right), \quad g^2 = \frac{\sqrt{2\mu E_b}}{8\pi\mu^2 \left( \arctan \left( \frac{\Lambda_0}{\sqrt{2\mu E_b}} \right) - \frac{\sqrt{2\mu E_b} \Lambda_0}{2\mu E_b + \Lambda_0^2} \right)}. \quad (12)$$

In the above expressions  $\mu$  is the reduced mass ( $\mu = m_D/2$ ),  $\Lambda_0$  is a cut-off parameter and  $E_b$  is the binding energy. We shall follow<sup>16</sup> and assume that  $\Lambda_0 = 1$  GeV. From<sup>16</sup> we see that one can compute the (dynamically generated) mass of a bound state and then determine its binding energy. Knowing  $\mu$ ,  $E_b$  and fixing  $\Lambda_0$ , we can use (12) to calculate  $\psi(0)$ . In what follows our reference value will be obtained using  $m_D = 1870$  MeV and the mass of the bound state equal to  $M_B = 3723$  MeV, as found in<sup>16</sup>. With these numbers we get  $E_b = 17$  MeV and  $|\psi(0)|^2 = 0.008$  GeV<sup>3</sup>.

The equivalent photon approximation is well known and it is described in several papers<sup>17</sup>. In general, when the photon source is a nucleus one has to use form factors and the calculation becomes somewhat complicated. Here we will follow<sup>18</sup> and define an UPC in momentum space. The distribution of equivalent photons generated by a moving particle with the charge  $Ze$  is<sup>18</sup>:

$$n(\mathbf{q}) d^3q = \frac{Z^2 \alpha}{\pi^2} \frac{(\mathbf{q}_\perp)^2}{\omega q^4} d^3q = \frac{Z^2 \alpha}{\pi^2 \omega} \frac{(\mathbf{q}_\perp)^2}{((\mathbf{q}_\perp)^2 + (\omega/\gamma)^2)^2} d^3q \quad (13)$$

where  $q$  is the photon 4-momentum,  $\mathbf{q}_\perp$  is its transverse component,  $\omega$  is the photon energy and  $\gamma$  is the Lorentz factor of the photon source ( $\gamma = \sqrt{s}/2m_p$  where  $m_p$  is the proton mass). To obtain the equivalent

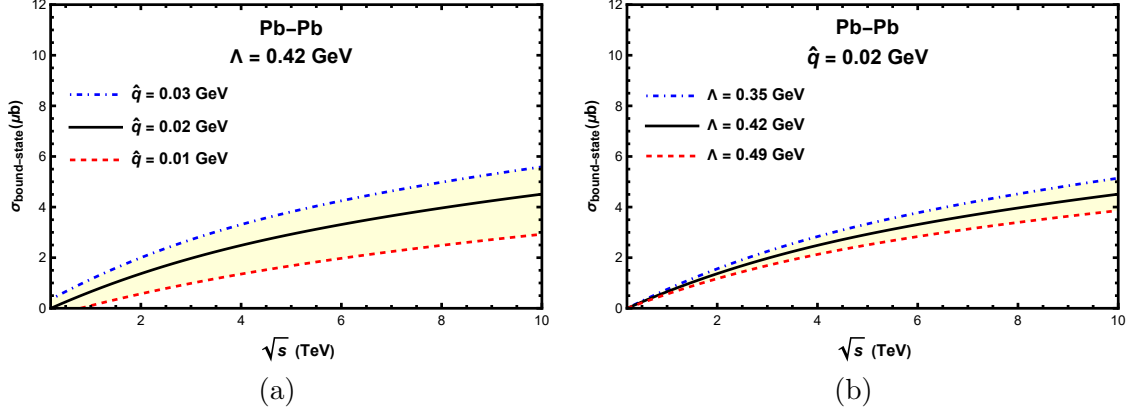


Figure 2 – Cross sections for  $D^+D^-$  bound state production as a function of the energy  $\sqrt{s}$ . a) Dependence on  $\hat{q}$  for fixed  $\Lambda$ . b) Dependence on  $\Lambda$  for fixed  $\hat{q}$ .

photon spectrum, one has to integrate this expression over the transverse momentum up to some value  $\hat{q}$ . The value of  $\hat{q}$  is given by  $\hat{q} = \hbar c/2R$ , where  $R$  is the radius of the projectile. For Pb,  $R \approx 7$  fm and hence  $\hat{q} \approx 0.014$  GeV. After the integration over the photon transverse momentum the equivalent photon energy spectrum is given by:

$$n(\omega)d\omega = \frac{2Z^2\alpha}{\pi} \ln\left(\frac{\hat{q}\gamma}{\omega}\right) \frac{d\omega}{\omega}, \quad (14)$$

Because of the approximations<sup>18</sup> the above distribution is valid when the condition  $\omega \ll \hat{q}\gamma$  is fulfilled. Using Eq. (14) we can compute the cross sections of free pair production,  $\sigma_P$ , and of bound state production,  $\sigma_B$ . They are given by:

$$\sigma_P(AA \rightarrow AA D^+ D^-) = \int_{m_D^2/\hat{q}\gamma}^{\hat{q}\gamma} d\omega_1 \int_{m_D^2/\omega_1}^{\hat{q}\gamma} d\omega_2 \sigma_P(\omega_1, \omega_2) n(\omega_1) n(\omega_2), \quad (15)$$

$$\sigma_B(AA \rightarrow AA B) = \int_{m_D^2/\hat{q}\gamma}^{\hat{q}\gamma} d\omega_1 \int_{m_D^2/\omega_1}^{\hat{q}\gamma} d\omega_2 \sigma_B(\omega_1, \omega_2) n(\omega_1) n(\omega_2), \quad (16)$$

where  $\sigma_P(\omega_1, \omega_2)$  and  $\sigma_B(\omega_1, \omega_2)$  are given by Eqs. (5) (with  $\hat{s} = 4\omega_1\omega_2$ ) and (11) respectively.

In Fig. 1b we show the cross sections for free pair production and compare it to the existing experimental data from LEP<sup>19</sup>. In fact, the LEP data are for  $e^+e^- \rightarrow e^+e^-c\bar{c}$ , i.e., the measured final states are  $D^+D^-$  and  $D^0\bar{D}^0$ . We assume that these two final states have the same cross section and, in order to compare with the data, we multiply our cross section  $\sigma(e^+e^- \rightarrow e^+e^-D^+D^-)$  by a factor two. In order to fit these data we will adapt expression (15) to electron-positron collisions. The  $\gamma\gamma \rightarrow D^+D^-$  cross section is the same but the photon flux from the electron (and also from the positron) and the integration limits are different<sup>1,17,18</sup>. Comparing our formula with these data, we determine the only parameter in the calculation, which is the cut-off  $\Lambda$ . In the figure, the curves are obtained substituting Eqs. (5) and (14) into (15). In the latter  $\hat{q} = m_e$ . The band is defined by the choice of two limiting values of  $\Lambda$ . In what follows we will use these values to estimate the uncertainty of our results.

In Fig. 2 we present the cross section for bound state production and study its dependence on  $\hat{q}$  (Fig. 2a)) and on  $\Lambda$  (Fig. 2b)). It is encouraging to see that at  $\sqrt{s_{NN}} \approx 5.02$  TeV we have:

$$\sigma(PbPb \rightarrow PbPb B) = 3.0_{-1.2}^{+0.8} \mu b \quad (17)$$

This number should be compared with results found in<sup>10</sup> and in<sup>20</sup>. In those papers, the production cross section of scalar states  $X(3940)$  and  $X(3915)$  in Pb Pb ultra-peripheral collisions at  $\sqrt{s_{NN}} = 5.02$  TeV were calculated and the results were in the range

$$5 \leq \sigma(PbPb \rightarrow PbPb R) \leq 11 \mu b \quad (18)$$

where  $R$  stands for  $X(3940)$  or  $X(3915)$ . These states are heavier than the one considered here but in both papers the X states were treated as meson molecules, as in the present work. It is reassuring to see that, in spite of the differences, the obtained cross sections are of the same order of magnitude.

### 3 Production of very forward pions

The magnetic field produced in relativistic heavy ion collisions is extremely strong<sup>21,22</sup>. A natural place to study the effects of this field is in ultra-peripheral relativistic heavy ion collisions<sup>1</sup>. Since there is no superposition of hadronic matter, the collision becomes essentially a very clean electromagnetic process.

In<sup>23</sup> it was argued that forward pions are very likely to be produced by magnetic excitation (ME) of the nucleons in the nuclei. The strong classical magnetic field produced by one nucleus induces magnetic transitions, such as  $N \rightarrow \Delta$  (where  $N$  is a proton or a neutron), in the nucleons of the other nucleus. The produced  $\Delta$  keeps moving together with the nucleus (or very close to it) and then decays almost exclusively through the reaction  $\Delta \rightarrow N + \pi$ . The produced pion has a very large longitudinal momentum and very large rapidity. Since there is no other competing mechanism for forward pion production in UPCs, the observation of these pions would be a signature of the magnetic excitation of the nucleons and also an indirect measurement of the magnetic field. In<sup>23</sup> it was shown that ME has a very large cross section. In<sup>24</sup> we proposed a way to test the classical approximation for the magnetic field. The process discussed in<sup>23</sup>,  $N \rightarrow \Delta \rightarrow N' \pi$ , was recalculated. In the quantum formalism the transition was induced by photons and not by the classical magnetic field. We computed the same process using a different formalism where the quanta of the field play the important role. We then compared the results obtained with the two formalisms. In this contribution we review the content of<sup>23</sup> and<sup>24</sup> and expand the discussion.

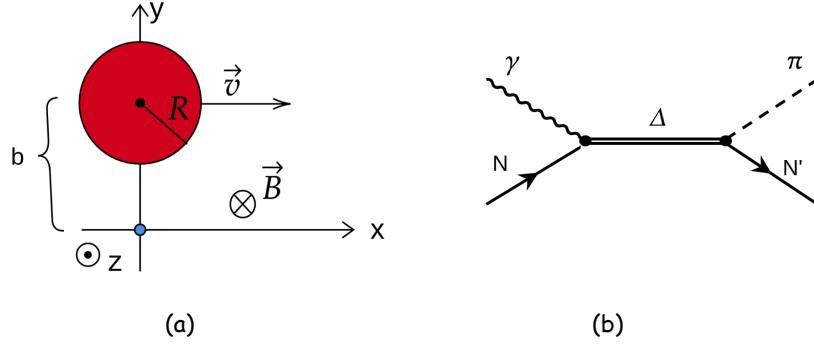


Figure 3 – a) Classical magnetic transition: a moving projectile creates a magnetic field  $\vec{B}$  which acts on the target at rest (at the origin of coordinates) flipping its spin. b) Quantum version of the same transition.

A strong magnetic field can convert a hadron into another one with a different spin, by “flipping the constituent quark spins”. Let us consider an ultra-peripheral  $Pb - p$  collision, where the proton is at rest, as shown in Fig. 3a. Under the influence of the strong magnetic field generated by the moving nucleus, the nucleon is converted into a  $\Delta$ . For the sake of definiteness let us consider the transition  $|p \uparrow\rangle \rightarrow |\Delta^+ \uparrow\rangle$ . The amplitude for this process is given by<sup>23</sup>:

$$a_{fi} = -i \int_{-\infty}^{\infty} e^{iE_{fi}t'} \langle \Delta^+ \uparrow | H_{int}(t') | p \uparrow \rangle dt' \quad (19)$$

where  $\hbar = 1$  and  $E_{fi} = (m_{\Delta}^2 - m_n^2)/2m_n$ , where  $m_{\Delta}$  and  $m_n$  are the  $\Delta$  and nucleon masses respectively. The interaction Hamiltonian is given by:

$$H_{int}(t) = -\vec{\mu} \cdot \vec{B}(t) \quad \text{with} \quad \vec{\mu} = \sum_{i=u,d} \vec{\mu}_i = \sum_{i=u,d} \frac{q_i}{m_i} \vec{S}_i \quad (20)$$

The magnetic dipole moment of the nucleon is given by the sum of the magnetic dipole moments of the corresponding constituent quarks,  $q_i$  and  $m_i$  are the charge and constituent mass of the quark of type  $i$  and  $\vec{S}_i$  is the spin operator acting on the spin state of this quark.

In Fig. 3a we show the system of coordinates, the moving projectile nucleus and target proton at the origin of the coordinates. We assume that the projectile-generated field is the same produced by a point charge. The field is given by<sup>23</sup>:

$$B_z(t) = \frac{1}{4\pi} \frac{qv\gamma(b-y)}{((\gamma(x-vt))^2 + (y-b)^2 + z^2)^{3/2}} \quad (21)$$

In the above expression  $\gamma$  is the Lorentz factor,  $b$  is the impact parameter along the  $y$  direction,  $v \simeq 1$  is the projectile velocity and the projectile electric charge is  $q = Ze$ . The interaction Hamiltonian acts on spin states. The relevant ones are:

$$|p \uparrow\rangle = \frac{1}{3\sqrt{2}}[udu(\downarrow\uparrow\uparrow + \uparrow\uparrow\downarrow - 2\uparrow\downarrow\uparrow) + duu(\uparrow\downarrow\uparrow + \uparrow\uparrow\downarrow - 2\downarrow\uparrow\uparrow) + uud(\uparrow\downarrow\uparrow + \downarrow\uparrow\uparrow - 2\uparrow\uparrow\downarrow)] \quad (22)$$

$$|\Delta^+ \uparrow\rangle = \frac{1}{3}(uud + udu + duu)(\uparrow\uparrow\downarrow + \uparrow\downarrow\uparrow + \downarrow\uparrow\uparrow) \quad (23)$$

With these ingredients we can compute the matrix element  $\langle\Delta^+ \uparrow|H_{int}|p \uparrow\rangle$ . It can be obtained by substituting Eq. (21) into Eq. (20) and then calculating the sandwiches of  $H_{int}$  with the spin states given above. The cross section for a single  $N \rightarrow \Delta$  transition is given by:

$$\sigma = \int |a_{fi}|^2 d^2b = 2\pi \int |a_{fi}|^2 b db \quad (24)$$

Inserting the matrix elements into (19) and using it in the above expression we find:

$$\sigma = \frac{Z^2 e^4}{9\pi m^2} \left(\frac{E_{fi}}{v\gamma}\right)^2 \int_R^\infty \left[K_1\left(\frac{E_{fi}b}{v\gamma}\right)\right]^2 b db \quad (25)$$

where  $K_1$  is the modified Bessel function. This is the result obtained with the semi-classical approach. For the purpose of comparison it is enough to consider a nucleon as a target. In<sup>23</sup> we computed the cross section for a nucleus-nucleus collision.

In the quantum formalism, the electromagnetic field produced by an ultra-relativistic electric charge is replaced by a flux of photons. Now, in a high energy UPC, the projectile becomes a source of almost real photons and we replace the classical field by a collection of quanta. Thus, the cross section of the process shown in Fig. 3b can be written in a factorized form in terms of the photon flux produced by the projectile and the photon-nucleon cross section<sup>1</sup>:

$$\sigma = \int \frac{d\omega}{\omega} n(\omega) \sigma_{\gamma N \rightarrow N\pi}(\omega) \quad (26)$$

In the above expression  $n(\omega)$  represents the photon spectrum generated by the source<sup>1</sup>:

$$n(\omega) = \frac{Z^2 \alpha}{\pi} \left[ 2\xi K_0(\xi) K_1(\xi) - \xi^2 [K_1^2(\xi) - K_0^2(\xi)] \right], \quad \xi = \frac{\omega(R_1 + R_2)}{\gamma} \quad (27)$$

where  $\omega$  is the photon energy,  $R_1$  and  $R_2$  are the radii of the projectile and the target, parametrized as  $R_A = 1.2 A^{1/3} fm$ , and  $\gamma$  the Lorentz boost in the target frame. From the above expression it is clear that the average energy carried by an emitted photon increases with  $\gamma$  and hence with the collision energy  $\sqrt{s}$ . In the LHC energy region  $\gamma \simeq 1000$  and the photon average energy  $\bar{\omega}$  may reach large values, such as  $\bar{\omega} \simeq 10$  GeV.

In order to perform the calculation of the total cross section, it is necessary to know the cross section of the process  $\gamma N \rightarrow N\pi$ . In a first approximation  $\sigma_{\gamma N \rightarrow N\pi}$  can be calculated evaluating the Feynman diagram shown in Fig. 3b. We need a formula which correctly reproduces the behavior of the cross section in the  $\Delta$  resonance region and which can be extrapolated to higher energies. This is the most important source of uncertainty in the evaluation of (26). A simple parametrization of the  $\pi^0$  photoproduction cross section can be taken from Jones and Scadron<sup>24</sup>. Knowing  $\sigma_{\gamma N \rightarrow N\pi}$ , we insert it into (26) and evaluate the cross section of the quantum process. The results are then compared with the results obtained with the semi-classical approach (given by (25)) and presented in Fig. 4. The cross sections are plotted as a function of the energy per nucleon (of the projectile) in the laboratory frame  $E_{Lab} = \gamma m_n$ . We compare the curves obtained with (25) (dashed line) and with (26) (solid lines). The band in the lower curve represents the different choices of the decay width  $\Gamma$ . The difference between the curves obtained with (25) and with (26) is small and reaches 9% at the highest energies. These results suggest that the classical approximation of the magnetic field reproduces most of the photon interaction in photoproduction in high energies.

The produced charged pions will be deviated by the dipole magnets which bend the colliding beams into the two separate beam pipes. However the neutral pions will not be bended by the magnetic field and will fly away following a tangent trajectory and reaching the zero degree calorimeters (ZDC's) which

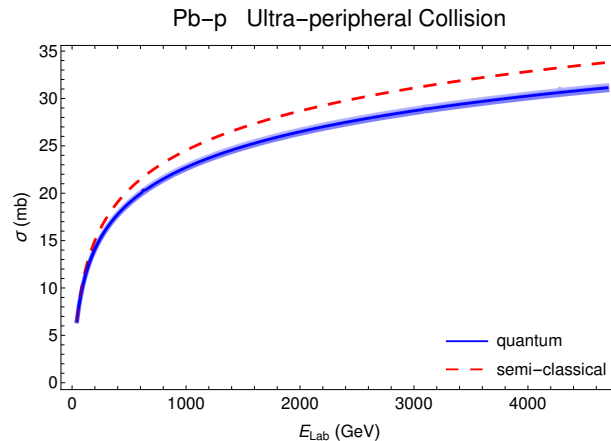


Figure 4 – Cross sections for pion production obtained with the semi-classical formalism, Eq.(25), dashed line, and with the quantum formalism, Eq. (26), solid line.

are part of both the ALICE and the ATLAS set up. They will be measured exactly in the same way as the ultra-forward neutrons produced in the electromagnetic dissociation processes already measured by the ALICE collaboration<sup>25</sup>. In fact, ultra-forward neutral pions have already been measured in proton-proton collisions at  $\sqrt{s} = 7$  TeV and in p-Pb collisions at  $\sqrt{s} = 5.02$  TeV by the LHCf collaboration<sup>26</sup> but no attempt was made to separate central from peripheral collisions. This might be done in the future.

#### 4 Conclusion

We have calculated the cross section for the production of a  $D^+D^-$  molecule in ultra-peripheral collisions. It is  $\sigma_B(AA \rightarrow AAB) = 3.0_{-1.2}^{+0.8} \mu b$  for  $\sqrt{s_{NN}} = 5.02$  TeV. This number is consistent with the results obtained for other scalar exotic charmonium molecules in Ref.<sup>10</sup> and in Ref.<sup>20</sup>. The parameters of the calculation are the hadronic form factor cut-off, the maximum transverse momentum of an emitted photon and the binding energy. All these parameters can be constrained by experimental information and/or by calculations and hence the precision of our calculation can be increased. The method used here can be easily applied to other exotic states.

We have also calculated the cross section for the production of very forward pions. We have used two methods, one with a classical magnetic field and the other with equivalent photons. Both methods yield a similar result: a quite large cross section for forward pion production. The neutral pions can in principle be measured. This would improve our knowledge about the validity of the classical approximation and about the strength of the magnetic field created in these collisions.

#### Acknowledgments

We are deeply indebted to K. Khemchandani and A. Martinez Torres for instructive discussions. This work was partially financed by the Brazilian funding agencies CNPq, CAPES, FAPESP, FAPERGS and INCT-FNA (process number 464898/2014-5). F.S.N. gratefully acknowledges the support from the Fundação de Amparo à Pesquisa do Estado de São Paulo (FAPESP).



## References

1. C. A. Bertulani, S. R. Klein and J. Nystrand, *Ann. Rev. Nucl. Part. Sci.* **55**, 271 (2005).
2. N. Brambilla, S. Eidelman, C. Hanhart, A. Nefediev, C.-P. Shen, C. E. Thomas, A. Vairo, and C.-Z. Yuan, *Phys. Rept.* **873**, 1 (2020); R. M. Albuquerque, J. M. Dias, K. P. Khemchandani, A. Martinez Torres, F. S. Navarra, M. Nielsen and C. M. Zanetti, *J. Phys. G* **46**, 093002 (2019).
3. T. W. Wu, Y. W. Pan, M. Z. Liu and L. S. Geng, *Sci. Bull.* **67**, 1735 (2022); [arXiv:2208.00882 [hep-ph]]; D. Marietti, A. Pilloni and U. Tamponi, *Phys. Rev. D* **106**, 094040 (2022). Pioneering studies were presented in S. J. Brodsky and F. S. Navarra, *Phys. Lett. B* **411**, 152 (1997).
4. P. Artoisenet and E. Braaten, *Phys. Rev. D* **83**, 014019 (2011); *Phys. Rev. D* **81**, 114018 (2010).
5. W. Lucha, D. Melikhov and H. Sazdjian, *Phys. Rev. D* **100**, 014010 (2019); *Phys. Rev. D* **98**, 094011 (2018).
6. R. D. Matheus, F. S. Navarra, M. Nielsen and R. Rodrigues da Silva, *Phys. Rev. D* **76**, 056005 (2007).
7. A. Esposito, E. G. Ferreira, A. Pilloni, A. D. Polosa and C. A. Salgado, *Eur. Phys. J. C* **81**, 669 (2021).
8. C. Bignamini, B. Grinstein, F. Piccinini, A. D. Polosa and C. Sabelli, *Phys. Rev. Lett.* **103**, 162001 (2009).
9. H. Zhang, J. Liao, E. Wang, Q. Wang and H. Xing, *Phys. Rev. Lett.* **126**, 012301 (2021); B. Wu, X. Du, M. Sibila and R. Rapp, *Eur. Phys. J. A* **57**, 122 (2021).
10. B. D. Moreira, C. A. Bertulani, V. P. Goncalves and F. S. Navarra, *Phys. Rev. D* **94**, 094024 (2016).
11. X. H. Cao, M. L. Du and F. K. Guo, [arXiv:2401.16112 [hep-ph]] and references therein.
12. P. Lebiedowicz, O. Nachtmann and A. Szczurek, *Phys. Rev. D* **98**, 014001 (2018).
13. M. E. Bracco, M. Chiapparini, F. S. Navarra and M. Nielsen, *Prog. Part. Nucl. Phys.* **67**, 1019 (2012).
14. An introduction to quantum field theory, M. Peskin and M. Schroeder, Addison-Wesley (1996), p. 150.
15. D. Gamermann, J. Nieves, E. Oset and E. Ruiz Arriola, *Phys. Rev. D* **81**, 014029 (2010).
16. C. W. Xiao and E. Oset, *Eur. Phys. J. A* **49**, 52 (2013).
17. G. Baur, K. Hencken, D. Trautmann, S. Sadovskiy and Y. Kharlov, *Phys. Rept.* **364**, 359 (2002).
18. M. I. Vysotskii and E. Zhemchugov, *Phys. Usp.* **62**, 910 (2019); [arXiv:1806.07238 [hep-ph]].
19. W. Da Silva [DELPHI], *Nucl. Phys. B Proc. Suppl.* **126**, 185 (2004); A. Csilling [OPAL], *AIP Conf. Proc.* **571**, 276 (2001). [arXiv:hep-ex/0010060 [hep-ex]].
20. R. Fariello, D. Bhandari, C. A. Bertulani and F. S. Navarra, *Phys. Rev. C* **108**, 044901 (2023).
21. V. Skokov, A. Y. Illarionov and V. Toneev, *Int. J. Mod. Phys. A* **24**, 5925 (2009).
22. V. Voronyuk et al., *Phys. Rev. C* **83**, 054911 (2011); C. S. Machado, F. S. Navarra, E. G. de Oliveira, J. Noronha and M. Strickland, *Phys. Rev. D* **88**, 034009 (2013).
23. I. Danhoni and F. S. Navarra, *Phys. Lett. B* **805**, 135463 (2020).
24. I. Danhoni and F. S. Navarra, *Phys. Rev. C* **103**, 024902 (2021).
25. B. Abelev, et al., ALICE Collaboration, *Phys. Rev. Lett.* **109**, 252302 (2012).
26. O. Adriani et al., LHCf Collaboration, *Phys. Rev. D* **94**, 032007 (2016).